Resonant Inelastic X-Ray Scattering of the Holon-Antiholon Continuum in $SrCuO_2$

Young-June Kim,[1] J. P. Hill,[1] H. Benthien,[2] F. H. L. Essler,[1] E. Jeckelmann,[3] H. S. Choi,[4] T. W. Noh,[4] N. Motoyama,[5] K. M. Kojima,[5] S. Uchida,[5] D. Casa,[6] and T. Gog[6]

[1]*Department of Physics, Brookhaven National Laboratory, Upton, New York 11973, USA*
[2]*Department of Physics, Philipps University Marburg, D-35032, Marburg, Germany*
[3]*Institute of Physics, University of Mainz, D-55099 Mainz, Germany*
[4]*ReCOE and School of Physics, Seoul National University, Seoul 151-747, Korea*
[5]*Graduate School of Frontier Sciences, University of Tokyo, Bunkyo, Tokyo 113-8656, Japan*
[6]*CMC-CAT, Advanced Photon Source, Argonne National Laboratory, Argonne, Illinois 60439, USA*

(Received 21 July 2003; published 2 April 2004)

We report a resonant inelastic x-ray scattering study of charge excitations in the quasi-one-dimensional Mott insulator $SrCuO_2$. We observe a continuum of low-energy excitations, the onset of which exhibits a small dispersion of $\sim$0.4 eV. Within this continuum, a highly dispersive feature with a large sinusoidal dispersion ($\sim$1.1 eV) is observed. We have also measured the optical conductivity, and studied the dynamic response of the extended Hubbard model with realistic parameters, using a dynamical density-matrix renormalization group method. In contrast to earlier work, we do not find a long-lived exciton, but rather these results suggest that the excitation spectrum comprises a holon-antiholon continuum together with a broad resonance.

DOI: 10.1103/PhysRevLett.92.137402 PACS numbers: 78.70.Ck, 71.10.Fd, 75.10.Pq, 78.30.–j

The separation of spin and charge degrees of freedom is one of the most important and fascinating properties of electrons in strongly correlated systems in one dimension. In particular, it is well known that, in the one-dimensional (1D) Hubbard model, the low-energy physics is dominated by collective excitations of decoupled charge and spin degrees of freedom called holons and spinons, respectively [1]. Experimentally, if one creates a hole by removing an electron, this hole is expected to decay into a spinon and a holon, which can be studied with angle resolved photoemission spectroscopy (ARPES) [2]. The situation is different for so-called "particle-hole" probes, such as optical spectroscopy, resonant inelastic x-ray scattering (RIXS), and electron energy-loss spectroscopy (EELS). In these experiments, the total charge is conserved in the scattering process, so that an electron is simply moved from one site to another, creating a hole and a doubly occupied site. The decay of the hole creates a holon and a spinon, while the double-occupancy decays into an antiholon and a spinon. Since photons and electrons strongly couple to the charge sector, the behavior of holon-antiholon pairs can be studied with these particle-hole probes [3,4].

The so-called corner-sharing chain cuprates Sr_2CuO_3 and $SrCuO_2$ are both charge-transfer insulators; that is, they have insulating gaps of $\sim$2 eV arising from strong electron correlations. Since their crystal structure is highly anisotropic, the electronic structure remains 1D over a wide temperature range. Only at a very low temperature does magnetic order set in, due to the small interchain coupling ($T_N \approx 2$ K for $SrCuO_2$ [5]). Based on the commonly used measure of quasi-one-dimensionality, $T_N/J \sim 10^{-3}$, these compounds can be regarded as among the best realizations of quasi-1D systems [6]. The quasi-1D nature of both $SrCuO_2$ and Sr_2CuO_3 has been studied extensively with various experimental techniques, including magnetic susceptibility [7], ARPES [2], Raman scattering [8], optical spectroscopy [9], EELS [3], RIXS [4], and neutron scattering [10].

In this Letter, we report a detailed study of the momentum dependence of the low-energy charge excitations in $SrCuO_2$, utilizing the RIXS technique. We observe a continuum of excitations arising from the creation of particle and hole pairs. Within this continuum, a well-defined spectral feature with a large sinusoidal dispersion ($\sim$1.1 eV) is observed. We have also measured the optical conductivity $\sigma(\omega)$ and carried out a dynamical density-matrix renormalization group (DDMRG) calculation of the extended Hubbard model. A comparison of the RIXS spectra with both the theoretical results and $\sigma(\omega)$ yields a consistent picture of charge excitations in this material: We find two dispersive spectral features. The first feature is the onset energy of the holon-antiholon continuum, which exhibits small dispersion ($\sim$0.4 eV). The second spectral feature is a more dispersive broad resonance that is the remnant of the strong-coupling exciton. This result contrasts earlier EELS work, in which the excitation spectrum was interpreted as being dominated by a bound exciton at large momenta [3].

In RIXS experiments, the incident x-ray energy is tuned to near the absorption edge of the particular element of interest, so that the inelastic scattering intensity of certain electronic excitations is resonantly enhanced. In addition, this gives an element specificity that is valuable in studying complex materials such as the cuprate compounds [4,11–14]. The RIXS experiments were carried out at the Advanced Photon Source on the undulator beam line 9IDB with the same setup used in previous

 © 2004 The American Physical Society

studies [14]. The scattering plane was vertical and the polarization of the incident x ray was kept perpendicular to the Cu-O plaquette. Note that the corner-sharing CuO_2 chain runs along the **c** direction. A single crystal of $SrCuO_2$ was grown using the traveling solvent floating zone method. The crystal was cleaved along the (0 1 0) plane and mounted on an aluminum sample holder at room temperature in an evacuated chamber.

In order to find the resonance condition, we first carried out a study of the incident energy (E_i) dependence of the RIXS intensity. There are two features that show resonance behavior in the energy-loss ($\omega \equiv E_i - E_f$) spectra, at $\omega \sim 3$ and $\omega \sim 6$ eV, respectively. The intensity of the 3 eV feature shows large enhancements at $E_i \approx 8982$ and $E_i \approx 8990$ eV, while the 6 eV feature is resonantly enhanced at $E_i \approx 8990$ and $E_i \approx 8996$ eV. We note that these three resonance energies correspond to the peaks in x-ray absorption spectra near the Cu K edge [15]. The intensity at 6 eV likely arises from both the Cu $K\beta_5$ emission and a charge-transfer-type excitation commonly found in the RIXS studies of cuprates [11,12]. Detailed studies of the E_i dependence will be reported elsewhere. Here we fix $E_i = 8982$ eV, and focus on the momentum dependence of the 3 eV feature.

Our main results are shown in Fig. 1, in which the RIXS intensity is plotted as a function of momentum and energy transfers. The pseudocolor scale of the observed intensity is shown on the right side in units of counts per second. The momentum transfer is shown in reduced units of $q/2\pi$ along the chain direction, and corresponds to the (0 11 q) position. Thus, $q/2\pi = -0.5$ is the 1D Brillouin zone boundary, while $q/2\pi = 0$ is the zone center. The lower cutoff of $\omega = 0.5$ eV shown in Fig. 1 is due to the large quasielastic contribution, and $\omega = 6$ eV is the upper limit of accessible energy transfer in this setup. The plotted intensity is the raw RIXS intensity without any absorption corrections. Almost constant factors were obtained from three different normalization methods [16], enabling us to compare the absolute intensities between different momentum transfers directly, except for $q/2\pi = -1$. The anomalously low overall intensity at $q/2\pi = -1$ arises from the very low angle of the incoming photons at this q.

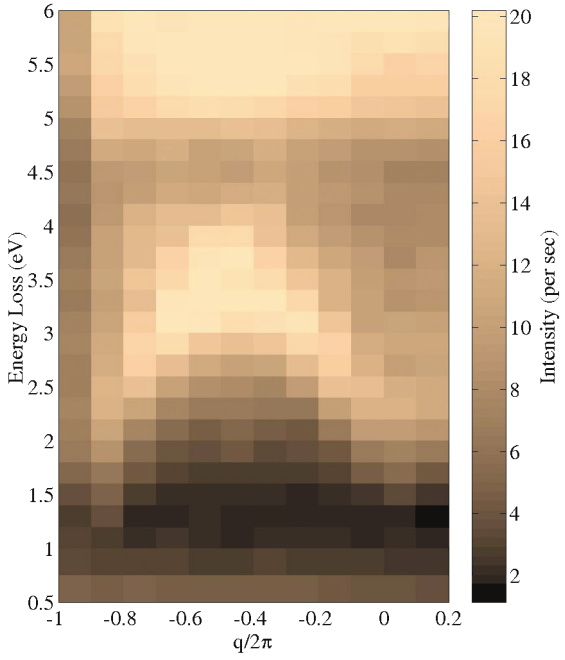

FIG. 1 (color). Pseudocolor plot of RIXS intensity as a function of momentum and energy transfer ($E_i = 8982$ eV).

The most prominent feature of the RIXS spectra shown in Fig. 1 is the highly dispersive feature at $\omega \approx 3$ eV. The momentum dependence of the peak position of this feature, shown in Fig. 2, exhibits a clear sinusoidal dispersion with a bandwidth of 1.1 eV. However, closer inspection of Fig. 1 reveals the presence of additional spectral weight on the low-energy side around $q/2\pi = -0.5$. This low-energy intensity around the zone boundary is evident for the $q = \pi$ data in Fig. 3, where the scattered intensity is plotted on a logarithmic scale. Since the momentum resolution at this position is about 0.1 reciprocal lattice units, it is unlikely that the additional low-energy intensity is due to a resolution effect. Thus, the best description of the observed spectra is that of a continuum of excitations, in which the dispersive feature resides. Note that this interpretation, particularly near $q = \pi$, is in contrast to previous EELS and RIXS results. In their EELS study of Sr_2CuO_3, Neudert *et al.* reported that the sharp spectral feature observed near $q = \pi$ is a bound exciton mode, due to a strong intersite Coulomb interaction [3]. The earlier RIXS study by Hasan *et al.* attributed the dispersive feature to the insulating gap edge [4]. Our RIXS results suggest that the continuum starts at much lower energy, and that the particle-hole pairs do not

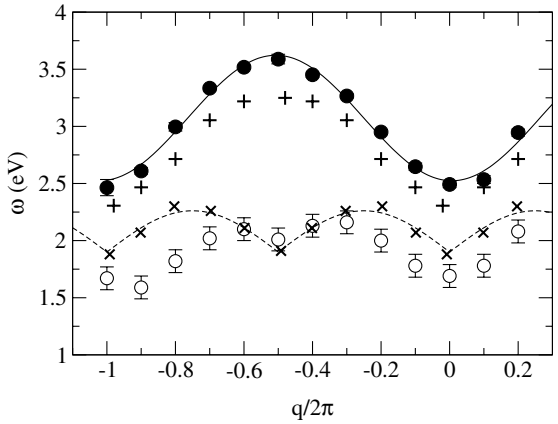

FIG. 2. The dispersion relation of the peak position (filled symbol) and the onset energy (open symbol) of the RIXS spectra. The solid line is $\omega(q) = 3.07 - 0.55\cos(q)$. Calculated peaks and onset energies in dynamical density-density correlation function, $\mathcal{N}(q, \omega)$, are also plotted as + and × symbols, respectively. The dashed line denotes the spinon dispersion relation as described in the text.

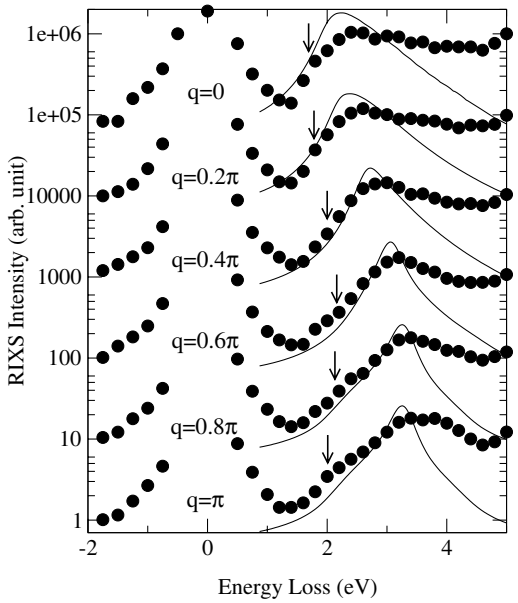

FIG. 3. Comparison of the RIXS spectra (circles) and $\mathcal{N}(q, \omega)$ (solid lines) at various momenta. To facilitate a direct comparison, $\mathcal{N}(q, \omega)$ is calculated with an experimental broadening of $\eta = 0.5t$ and divided by $\sin^2(q/2)$. Arrows denote the onset of the RIXS spectral weight.

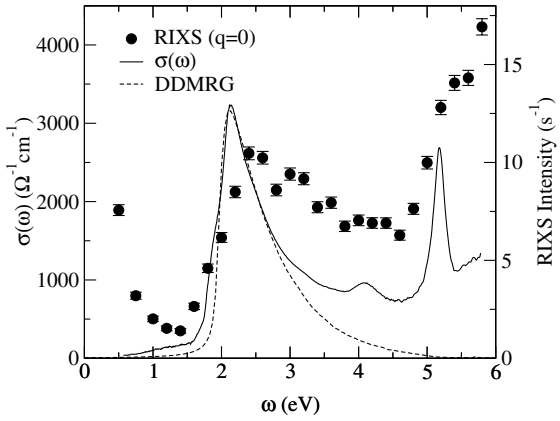

FIG. 4. The optical conductivity $\sigma(\omega)$ at $T = 90$ K is plotted as a solid line, and compared with RIXS spectra obtained at the zone center. The dashed line is the DDMRG calculation of $\sigma(\omega)$ with an experimental broadening of $\eta = 0.1t$.

form a bound exciton at $q = \pi$. The onset energy of the spectral weight extracted from each scan is shown in Fig. 3 as an arrow. The dispersion of these onset energies is plotted in Fig. 2. Note that the bandwidth of the onset energy dispersion ($\sim$0.4 eV) is much smaller than that of the peak position, as discussed later.

In concert with the RIXS data, we have also studied the optical properties of $SrCuO_2$, measuring the reflectivity of a cleaved surface between 6 meV and 6 eV, with the polarization along the **c** axis. Optical conductivity, $\sigma(\omega)$ calculated from the reflectivity data using the Kramers-Kronig relation with an anchoring process, is plotted as a solid line in Fig. 4 and compared with the $q = 0$ RIXS data. The validity of the Kramers-Kronig calculation was checked by directly measuring the complex dielectric function with an ellipsometry method. In the frequency range of interest ($1 \sim 4$ eV), identical spectra were obtained from both techniques. The $q = 0$ RIXS data are expected to be different from that of $\sigma(\omega) = \omega\,\mathrm{Im}[\epsilon(0, \omega)]$, since the response function measured in RIXS is believed to be close to a dielectric loss function, $\mathrm{Im}[-1/\epsilon(q, \omega)]$. Instead, one should focus on the onset energy of the spectral weight, which should be independent of both the particular response function being measured and matrix-element effects. Both the RIXS data and the $\sigma(\omega)$ main feature exhibit onset energies around 1.7 eV, which correspond to the continuum edge at the zone center.

To understand the observed continuum and the dispersive spectral feature, we have studied a simple one-band half-filled 1D extended Hubbard model (EHM) [17–20], in which the nearest-neighbor repulsion V is explicitly included, in addition to the usual t and U. It is clear that a full theoretical description of $SrCuO_2$ requires a multiband model based on the Cu $3d$ and O $2p$ orbitals. However, a precise and reliable determination of dynamical correlation functions in such models is still a formidable challenge. Several previous studies suggested that much of the essential physics of both Sr_2CuO_3 and $SrCuO_2$ at low energies can be captured by the EHM [3,17–20]. We have therefore used a DDMRG algorithm [20] to determine the optical conductivity and density response function in this model for realistic values of U and V on chains of up to 128 sites. All previous studies either dealt with unrealistic parameter values [3] or suffered from severe finite-size effects caused by the very small system sizes amenable to exact diagonalization methods [21].

The parameters t, U, and V of the EHM were fixed by comparing DDMRG calculations of the optical conductivity $\sigma(\omega)$ to the experimental data and requiring compatibility with the value $J \approx 0.23$ eV for the Heisenberg exchange coupling J obtained from neutron scattering [10]. As shown in Fig. 4, an excellent fit for the low-energy peak in $\sigma(\omega)$ is obtained for $t = 0.435$ eV, $V/t = 1.3$, and $U/t = 7.8$. For these values, we obtain $J \approx 0.24$ eV from both $1/U$ expansions and DDMRG computations of the spinon dispersion in the single-particle spectral function. Note that the calculated $\sigma(\omega)$ in Fig. 4 agrees with the measured spectra on an absolute scale.

The excitation spectrum of the EHM with these parameters consists of scattering states of gapped, spinless charge $\mp e$ collective modes [(anti)holons] and of gapless, chargeless spin $\pm 1/2$ collective modes (spinons). In contrast to the strong-coupling results reported in Ref. [17], no excitonic excitations are found in any part of the Brillouin zone. The current operator is charge neutral and, hence, only excitations with equal numbers of

holons and antiholons contribute to $\sigma(\omega)$. Most of the spectral weight of the low-energy peak in $\sigma(\omega)$ is attributed to excited states with one holon and one antiholon each. The contributions of the spin degrees of freedom to $\sigma(\omega)$ is small [19].

The RIXS data are more difficult to model as at present there is no completely satisfactory theory of RIXS. However, it is clear that the RIXS process involves charge fluctuations that may be represented by the low-energy excitations of the EHM [4,12,18]. We have therefore determined the dynamical density-density correlation function $\mathcal{N}(q, \omega)$ by DDMRG. The results are shown in Fig. 3 as solid lines. At small momenta $\mathcal{N}(q, \omega)$ is proportional to q^2 and, thus, we use a normalization factor of $\sin^2(q/2)$ to compare $\mathcal{N}(q, \omega)$ at various momenta. We note that *on a lattice* the Fourier transform $V(q)$ of the Coulomb potential is approximately given by $1/\sin^2(q/2)$. Therefore, the renormalized $\mathcal{N}(q, \omega)$ in Fig. 3 is probably close to the dielectric loss function $\mathrm{Im}[-1/\epsilon(q, \omega)] \propto V(q)\mathcal{N}(q, \omega)$ of the EHM. At $q = 0$, there is a broad "band" of states with a peak around 2.3 eV. As we move towards the zone boundary, this feature narrows significantly. Importantly, however, even at $q = \pi$ the peak has an intrinsic width; that is, it is not a long-lived exciton mode. Furthermore, there is sizable intensity below the peak at $q = \pi$. This is in contrast to the strong-coupling $U \to \infty$ limit [17], where $\mathcal{N}(q \approx \pi, \omega)$ is dominated by an excitonic holon-antiholon bound state. Our interpretation is that, as U is reduced to smaller, more realistic values, the exciton acquires a finite lifetime and turns into a broad holon-antiholon resonance.

Let us try to relate these findings to the RIXS data. In Fig. 3, the normalized $\mathcal{N}(q, \omega)$ is directly compared with the RIXS spectra at equivalent q positions. The onset of the RIXS spectrum shown in Fig. 3 seems to lie in the area where $\mathcal{N}(q, \omega)$ begins to show appreciable spectral weight. The onset energy of $\mathcal{N}(q, \omega)$ is plotted in Fig. 2 as a function of q (crosses). The onset dispersion of $\mathcal{N}(q, \omega)$ follows the dashed line, which is the single-spinon dispersion relation shifted by a constant energy: $\frac{\pi}{2}J|\sin(q)| + 1.9$. This spinonlike dispersion of the onset energy of $\mathcal{N}(q, \omega)$ is consistent with the low-energy field theory prediction [22]. Qualitative features of this spinonlike dispersion of the onset energy of $\mathcal{N}(q, \omega)$ appear to be consistent with features of the RIXS data (open circles, Fig. 2), such as the bandwidth of $\sim\pi J/2$, and the $q = \pi$ point being a local minimum. In addition, we have compared the dispersion of the peak positions. As indicated in Fig. 2, the peak dispersion in $\mathcal{N}(q, \omega)$ is very similar to that of the RIXS data. However, such a quantitative agreement between the RIXS peak positions and $\mathcal{N}(q, \omega)$ may well be coincidental, and further calculation of the full RIXS response function is necessary to draw any firm conclusions.

In summary, we have studied the energy and momentum dependence of low-energy charge excitations in quasi-1D $SrCuO_2$, using both optical spectroscopy and resonant inelastic x-ray scattering. We observe a continuum of excitations which we associate with the creation of holon and antiholon pairs. The onset of the holon-antiholon continuum exhibits spinonlike dispersion. Within this continuum, a well-defined spectral feature with a large sinusoidal dispersion is also observed. By comparing the observed spectra with a DDMRG calculation of 1D EHM, we interpret this well-defined feature as a broad holon-antiholon resonance due to the intersite Coulomb interaction. In contrast to earlier studies, we find that the holon-antiholon pairs do not form an exciton, and the continuum starts at much lower energy than previously reported.

We would like to thank F. Gebhard and C. C. Homes for invaluable discussions. The work at Brookhaven was supported by the U.S. DOE, under Contract No. DE-AC02-98CH10886. Use of the Advanced Photon Source was supported by the U.S. DOE, under Contract No. W-31-109-Eng-38. H. B. acknowledges support by Optodynamics Center of the Philipps-Universität Marburg and thanks the Institute for Strongly Correlated and Complex Systems at BNL for hospitality and support.

[1] E. L. Lieb and F. Y. Wu, Phys. Rev. Lett. **20**, 1445 (1968).
[2] C. Kim *et al.*, Phys. Rev. Lett. **77**, 4054 (1996); Phys. Rev. B **56**, 15 589 (1997).
[3] R. Neudert *et al.*, Phys. Rev. Lett. **81**, 657 (1998).
[4] M. Z. Hasan *et al.*, Phys. Rev. Lett. **88**, 177403 (2002).
[5] M. Matsuda *et al.*, Phys. Rev. B **55**, 11 953 (1997).
[6] M. Steiner, J. Villain, and C. G. Windsor, Adv. Phys. **25**, 87 (1976).
[7] N. Motoyama, H. Eisaki, and S. Uchida, Phys. Rev. Lett. **76**, 3212 (1996).
[8] O. V. Misochko *et al.*, Phys. Rev. B **53**, 14 733 (1996).
[9] Z. V. Popovic *et al.*, Phys. Rev. B **63**, 165105 (2001).
[10] I. A. Zaliznyak (unpublished).
[11] J. P. Hill *et al.*, Phys. Rev. Lett. **80**, 4967 (1998).
[12] P. Abbamonte *et al.*, Phys. Rev. Lett. **83**, 860 (1999).
[13] M. Z. Hasan *et al.*, Science **288**, 1811 (2000).
[14] Y. J. Kim *et al.*, Phys. Rev. Lett. **89**, 177003 (2002).
[15] J. M. Tranquada *et al.*, Phys. Rev. B **44**, 5176 (1991).
[16] We considered normalization schemes based on elastic intensity, energy gain background ($\omega \ll 0$), and the fluorescence yield.
[17] W. Stephan and K. Penc, Phys. Rev. B **54**, R17 269 (1996).
[18] K. Tsutsui, T. Tohyama, and S. Maekawa, Phys. Rev. B **61**, 7180 (2000).
[19] F. H. L. Essler, F. Gebhard, and E. Jeckelmann, Phys. Rev. B **64**, 125119 (2001).
[20] E. Jeckelmann, Phys. Rev. B **67**, 075106 (2003).
[21] A. Hübsch *et al.*, Phys. Rev. B **63**, 205103 (2001).
[22] D. Controzzi and F. H. L. Essler, Phys. Rev. B **66**, 165112 (2002).